Published in final edited form as:

Sci Transl Med. 2015 January 28; 7(272): 272ra11. doi:10.1126/scitranslmed.aaa1616.

Regulation of dendrimer:dextran material performance by altered tissue microenvironment in inflammation and neoplasia

Nuria Oliva[1,#], **Maria Carcole**[1,2,#], **Margarita Beckerman**[1,3], **Sivan Seliktar**[1,3], **Alison Hayward**[4], **Butch Stanley**[4], **Nicola Maria Anne Parry**[5], **Elazer R. Edelman**[1,6], and **Natalie Artzi**[1,7,*]

[1]Institute for Medical Engineering and Science, Massachusetts Institute of Technology (MIT), Cambridge, MA 02139, USA

[2]Department of Chemistry, Institut Quimic de Sarrià, Universitat Ramon Llull, Barcelona 08017, Spain

[3]Ort Braude College, Karmiel 21982, Israel

[4]Concord Biomedical Sciences and Emerging Technologies, Lexington, MA 02421, USA

[5]Division of Comparative Medicine, Massachusetts Institute of Technology, Cambridge, MA 02139, USA

[6]Cardiovascular Division, Department of Medicine, Brigham and Women's Hospital, Harvard Medical School, Boston, MA 02115, USA

[7]Department of Anesthesiology, Brigham and Women's Hospital, Harvard Medical School, Boston, MA 02115, USA

Abstract

[*]Corresponding author: nartzi@mit.edu.
[#]Denotes equal contribution.

SUPPLEMENTARY MATERIALS

www.sciencetranslationalmedicine.org/cgi/content/full/7/272/272ra11/DC1

Fig. S1. Dendrimer:dextran interfacial morphology characterization in inflammation and neoplasia.
Fig. S2. Collagen I immunostaining in healthy and neoplastic tissues.
Fig. S3. Study of alterations in tissue biological and chemical cues as a function of disease severity.
Fig. S4. *En face* collagen I correlations with neutrophil recruitment and microspheres conjugation.
Fig. S5. In vivo hematoxylin and eosin (H&E) staining images.
Table S1. Tabulated data from Fig. 1, C and D
Table S2. Tabulated data from Fig. 1E
Table S3. Tabulated data from Fig. 1F
Table S4. Tabulated data from Fig. 2A
Table S5. Tabulated data from Fig. 2B
Table S6. Tabulated data from Fig. 4B
Table S7. Tabulated data from Fig. 4C
Table S8. Tabulated data from Fig. 4D
Table S9. Tabulated data from Fig. 4E

Competing interests: N.O., M.C., N.A., and E.R.E. hold a patent on Biocompatible Adhesive Materials and Methods (U.S. 8,802,072 B2). The other authors declare that they have no competing interests.

Author contributions: N.O. designed and performed all experiments and wrote the paper; M.C., M.B., and S.S. helped perform experiments; A.H. performed animal enterotomy surgeries; B.S. and N.M.A.P performed histology scoring, and E.R.E. and N.A. provided funding and wrote the paper.

A “one material fits all” mindset ignores profound differences in target tissues that affect their responses and reactivity. Yet little attention has been paid to the role of diseased tissue on material performance, biocompatibility, and healing capacity. We assessed material-tissue interactions with a prototypical adhesive material based on dendrimer:dextran and colon as a model tissue platform. Adhesive materials have high sensitivity to changes in their environment and can be exploited to probe and quantify the influence of even subtle modifications in tissue architecture and biology. We studied inflammatory colitis and colon cancer and found, not only a difference in adhesion related to surface chemical interactions, but also the existence of a complex interplay that determined the overall dendrimer:dextran biomaterial compatibility. Compatibility was contextual, not simply a constitutive property of the material, and was related to the extent and nature of immune cells in the diseased environment present prior to material implantation. We then showed how to use information about local alterations of the tissue microenvironment to assess disease severity. This in turn guided us to an optimal dendrimer:dextran formulation choice using a predictive model based on clinically relevant conditions.

INTRODUCTION

Biomaterials are increasingly used to support or reprogram their complex biological microenvironment by either providing structural stability and mechanical restoration or by serving as scaffolds for local drug release or for embedding of cells. Further, materials have been functionalized with biological sequences of natural components to attract reparative endogenous cells and modulate their phenotypes (1–5). Despite the use of such materials in injured, inflamed, or diseased environments, little has been reported about the impact of disease on the material itself and whether the material performs its intended action in selected environments. Materials with adequate efficacy in a healthy environment might demonstrate suboptimal performance and altered host-material responses in diseased settings. Although the inflammatory response to material exposure follows an orderly sequence of events, preexisting processes such as inflammation might set this order awry. The sequence of early neutrophil invasion followed by macrophage infiltration and eventually the formation of foreign-body giant cells is modified in a disease state (6). Disease alters the basal immune state, as immune cells are present at the site of injury well before any material is implanted. Such is the case of inflammatory diseases, in which the preexisting tissue reactivity might alter tissue response to a material. We envisioned that rational development of materials with optimal healing capacity can be enabled only in the context of the intended clinical use of the material and with a deep understanding of the local environment.

We used the gastrointestinal tract as a model system to study the impact of disease on the tissue microenvironment and two disease models—inflammation and neoplasia—which we surmised would span a range of cellular responses and a spectrum of reactions to a material. Adhesive materials are ideal candidates with which to study the effects of gut disease on performance given their intimate interaction with tissue in this defined locale and their clinical relevance in mediating complications associated with leakage after surgical gut repair (7). We recently showed that adhesive dendrimer:dextran-based materials facilitate the probing of local changes in tissue surface chemistry by virtue of their distinct

interactions with different target tissues (7, 8). Here we exploit this feature to examine, in our model systems, the effects of disease-driven alterations in local tissue-state on the tissue microenvironment and the clinical implications of such alterations. We show that carcinogenesis and inflammation of the colon are two distinct processes that present substantially different surfaces—driven by their biochemistry and cell biology—to the external environment. Interaction of the dendrimer:dextran material with tissue surfaces and tissue responses to this adhesive material were altered in a disease type– and pathological state–dependent manner. The interrelationship between material science and tissue biology should be considered as we seek to facilitate predictive and controlled material performance in specific clinical scenarios. Concepts learned from these studies might illuminate general guidelines by which to assess material-tissue interactions and their disease-driven alterations.

RESULTS

Characterization of tissue surface chemistry and material performance in colon cancer and colitis

We used two different animal models for studying the impact of local pathology on dendrimer:dextran performance across species and recapitulated the chemical, structural, and biological cues characteristic of a particular disease in a specific location. We used a commercially available rat orthotopic model for colon cancer and developed a colitis model in rabbits that provided sufficient tissue biopsies to conduct mechanical testing, characterize tissue chemistry, and build a predictive model that informs material choice for each disease severity.

Dextran aldehyde reacts internally with dendrimer amines to form a hydrogel and with tissue amines to provide adhesion. To understand the extent to which tissue surface chemistry was altered by cancer or colitis in our model systems, we quantified the interaction of aldehyde-coated microspheres with healthy and diseased tissues as a measure of tissue-amine binding sites. We hypothesized that microsphere adhesion in colon cancer would exhibit alterations in concert with changes in tissue surface amine density. Indeed, a significant increase in amine density was detected with fluorescent aldehyde-coated microspheres in cancerous colon tissue (Fig. 1A, i–ii), which displayed a greater number of chemical groups that were available for material interaction. A concomitant increase in material adhesion (Fig. 1A, iii–iv) was detected by fluorescence intensity at the interfacial region (defined as the area of the biomaterial that interacts with the tissue and has a morphology distinct from the rest of the material (fig. S1, a and b). Smaller and fewer pores of reduced area (U=interfacial pores area) were present within a narrower interfacial region [W= interfacial width; W= 104.7 ± 20.8 μm and U = $5.85\times10^{2} \pm 7.77\times10^{1}$ μm^2 for cancerous rat tissue and W= 130.3 ± 27.9 μm and U = $5.44\times10^{3} \pm 1.75\times10^{3}$ μm^2 for healthy rat tissue; fig. S1, c and d; $P<0.05$ by two-tailed *t*-test for independent samples], which indicated that interfacial adhesion and integration of the material were enhanced. Macroscopic-force measurement of adhesion failure (as determined with a mechanical tester, see Materials and Methods) rose 43% (from 0.566 ± 0.08 N to 0.808 ± 0.04 N) for colon cancer tissue compared to healthy colon tissue (Fig. 1C, $P<0.05$, by two-tailed *t*-test for independent samples; data tabulated in table S1).

This increase in maximum load correlated with observed microscopic changes, as indicated by higher interfacial fluorescence and amine density.

In contrast, amine density was lower in inflammatory colitis compared to the healthy state (Fig. 1B, i–ii). Material-tissue adhesion was reduced in colitis tissue (Fig. 1B, iii–iv and fig. S1e) as indicated by a wider interfacial region as well as a higher pore area (W=216.3 ± 37.5 μm and U=$1.39\times10^4 \pm 2.84\times10^3$ μm^2) compared with that of healthy colon tissue (W=108.3 ± 38.6 μm and U=$3.40\times10^3 \pm 1.13\times10^3$ μm^2; fig. S1, f and g; $P<0.05$ by two-tailed *t*-test for independent samples). The reduction in tissue binding sites, indicated by microsphere conjugation, translated into inferior material adhesion strength as corroborated by a 58% reduction in the mechanical load required to break the bond between the colitic tissue and our material relative to the healthy state (from 0.812 ± 0.16 N to 0.34 ± 0.13 N, respectively) (Fig. 1D, $P<0.05$ by two-tailed *t*-test for independent samples; data tabulated in table S1).

We then examined whether dendrimer:dextran formulation protocols can compensate for the reduced availability of tissue binding sites in colitis. Material composition spanned a wide range of adhesion strengths (Fig. 1E; data tabulated in table S2). As dextran aldehyde solid content was increased from 7.5 to 25 wt%, maximal load at failure increased 235% (from 0.25±0.03 N to 0.83 ±0.22 N, $P<0.05$ by two-tailed *t*-test for independent samples) (7, 9). The excess aldehydes provided by raises in the dextran aldehyde solid content increased the probability for material interaction with tissue amines. Indeed, by increasing dextran aldehyde solid content from 10 wt% in healthy tissue to 25 wt% in the case of colitis, we were able to compensate for the reduction in tissue amine density in the disease state and achieve the same level of adhesion strength as in the healthy state (Fig. 1F; data tabulated in table S3).

Determination of diseased-tissue surface chemistry by collagen quantification

To understand the underlying mechanism that mediated tissue surface chemistry modifications in the context of cancer and colitis, we characterized the primary tissue proteins in healthy and diseased tissues. Collagen I accounts for ~70% of the total collagen in gastrointestinal tissues (10). Using cryosectioned tissue, we measured a significant increase in collagen content in vitro in the presence of neoplasia (fig. S2). The same trend was observed when we quantified collagen and bound microspheres on healthy and cancerous tissue surfaces (*en face*) with an in vivo imaging system. These findings suggest that a higher number of amine groups reside on the surface of cancerous versus healthy colon tissue (Fig. 2A; data tabulated in table S4).

In contrast, inflammation is known to result in collagen degradation and tissue surface remodeling as a consequence of the release, by neutrophils, of factors that activate matrix metalloproteinases such as MMP-8 (also known as collagenase-2 or neutrophil collagenase). We hypothesized that disease-driven changes in collagen levels on the surface of the gut lumen, where the disease originates, would disseminate to the external surface of the gut—the serosa (peritoneum-facing)—where the material is applied. If this is the case, then alteration of tissue serosal surface chemistry would affect material performance.

To examine this hypothesis, we induced colitis in rabbits by instilling 2,4-dinitrobenzenesulfonic acid (DNBS) intra-colonially and tested whether collagen content and hence, amine concentration varied on the serosal side of the gut (Fig. 2, B and C). We observed a reduction in collagen content throughout the three layers of the intestinal wall of colitic tissue (Fig. 3A, i and iii), and this effect disseminated to the serosal layer, as evident by the reduction in *en face* collagen content (Fig. 3A, iv–vi) and in microsphere conjugation (Fig. 2B; data tabulated in table S5). There was a strong linear correlation (R^2=0.99, Fig. 2C) between serosal *en face* collagen I content and serosal tissue amines (as measured by microspheres conjugation), and this relation was maintained across species (rats and rabbits; Fig. 2C).

Deciphering the impact of disease severity on tissue microenvironment

Colitis presents clinically as a range of severities. We investigated whether differential luminal degrees of inflammation would disseminate to the serosal side in a disease-severity dependent manner. We instilled various concentrations of DNBS into rabbit colons to achieve a range of disease severities and then validated our model through quantification of tumor necrosis factor alpha (TNF-α and neutrophil recruitment in the gut (fig. S3a, i–vi). TNF-α is known to be upregulated in inflammatory bowel disease in humans (11) because it is released in the context of inflammation by immune-surveillance macrophages present in the mucosal layer of the colon (12). TNF-α upregulation then leads to neutrophil recruitment to the gut mucosa, tissue infiltration and subsequent release of MMP-8, which degrades collagen in the basement membrane (13). Indeed, TNF-α release increased over a 7.4-fold range (from 30.9 ± 8.57 to 229.2 ±27.67 in relative fluorescence) with the severity of induced colitis, while neutrophils recruitment was increased in a correlative manner (5.5-fold; from 10.7 ± 13.51 to 60.4 ± 5.93 in relative fluorescence) (fig. S3b). As a result, we observed a correlative 1.7-fold decrease in basement-membrane collagen (from 336.6 ± 8.05 to 218.7 ± 15.65 in relative fluorescence) (Fig. 3A, i–iii, fig. S3b).

We also observed a linear correlation between *en face* collagen content in the serosa (Fig. 3A, iv–vi) and the extent of inflammation, as measured by the recruitment of neutrophils to the gut, thus corroborating the transmural nature of this disease in our rabbit model (fig. S4a, R^2=0.97). This decrease in serosal collagen level was further supported by a decrease in surface amine density, which correlated linearly with serosal collagen content (fig. 4b, R^2=0.94). These findings suggest that one can use the rapid measure of surface amine density to guide one's choice of adhesive properties in a dendrimer:dextran material in a way that is clinically relevant and yields information on disease severity. Such properties might facilitate a more personalized selection of materials for colitis treatment than is currently possible.

Building a predictive model to guide material choice

Colitic tissues with different degrees of inflammation were tested for amine density and adhesion strength using three different material formulations of varying aldehyde content (10%, 15%, and 20%). For a particular formulation, adhesion strength decreases with disease severity in a linear fashion. As we increase dextran aldehyde solid content, the slope of this curve increases, indicating higher adhesion strength (Fig. 3B). Interestingly, there is a

linear correlation between the slope of these curves and dextran solid content (R^2=0.99, Fig. 3C). Hence, we can predict adhesion strength of a new formulation for any disease state using these relationships. Indeed, there was an excellent agreement between the calculated and predicted adhesion strengths of 25% dextran aldehyde formulation applied to tissue surfaces that are healthy, or with mild and severe colitis (R^2=0.99, with errors smaller than 6%, Fig. 3D). We envision performing rapid assessment of amine density in the operating room on patients' biopsies to guide surgeons on the optimal material formulation to be used, in a patient-specific manner, such that adequate adhesion will be achieved.

Evaluation of material biocompatibility and healing capacity in vivo

We examined inflammation in the implant area as well as biological response to a dendrimer:dextran material (serosal heterophils) and healing capacity (serosal fibrosis) compared to use of sutures in vivo for healthy compared to colitic or cancerous tissues. Healthy rat colonic tissue appeared normal in structure (Fig. 4A, i and fig. S5a, i–iii), and the colorectal cancer rat model verified the existence of a mass of abnormal tissue with differentiated cells forming the tumor (Fig. 4A, ii and fig. S5a, iv–vi). Similarly, healthy rabbit colonic tissue appeared normal with intact mucosal and serosal layers (Fig. 4A, iii and fig. S5b, i–iii), while colitic tissue presented as diffusely necrotic mucosa with an intense heterophilic inflammatory response (Fig. 4a, iv and fig. S5b, iv–vi).

The levels of inflammation were not statistically distinguishable when dendrimer:dextran material was applied to the serosal layer of lacerated healthy or cancerous tissue in the presence or absence of the adhesive (Fig. 4, B and C). The difference in heterophil (that is, granular leukocytes) recruitment to the serosal layer was not statistically significant when sutures alone were used compared to sutures plus adhesive, both in healthy and cancerous states (Fig. 4, B and C). Serosal fibrosis was similar with and without adhesive application in healthy tissue (Fig. 4B; data tabulated in table S6). When sutures alone were applied, tissue fibrosis was reduced in the cancerous state compared to the healthy state. Application of adhesive material to cancerous tissue improved healing to levels comparable to those of healthy tissue, as measured by serosal fibrosis (Fig. 4C; data tabulated in table S7). Colitic tissue presents with higher total inflammation whether sutures alone or sutures plus material were applied, owing to the nature of the disease (Fig. 4E; data tabulated in table S9). The immune response to dendrimer:dextran was contextual; the number of serosal heterophils in lacerated healthy tissue was not altered upon material application to the serosal layer; in contrast, the difference in serosal heterophil numbers upon material application was statistically significant in the colitic state compared to sutures alone (Fig. 4, D and E; data tabulated in table S8). Similar to what was observed in the cancerous model, healing capacity (as measured by serosal fibrosis) after material application to the serosal layer in colitic tissue was improved compared to that of suture application alone, while healthy tissue presented good repair capacity irrespective of whether the adhesive material was used or not (Fig. 4, D and E).

DISCUSSION

Variations in tissue surface chemistry between different tissue surfaces dictate their interaction with our adhesive material in healthy states (7, 8). We showed herein that tissue surface chemistry was modified to an even greater extent by local pathology relative to variations between different tissues in the healthy state. Pathological states exerted profound effects on tissue:biomaterial interactions and material performance for dendrimer dextran adhesive hydrogel. Tissue surface chemistry (amine content) and the biological microenvironment were significantly altered in the face of inflammation and neoplasia.

To understand the impact of tissue surface modification by a disease on dendrimer:dextran material performance, we quantified surface collagen levels as a predictive measure for adhesion strength. Amino acids from structural proteins are the main anchoring points for amine-reactive adhesives and thus can be used to define adhesion strength. We used serosal collagen I as a measure for assessing amine density because it comprises ~70% of all collagen and is the most prevalent protein in the gastrointestinal tract. Colorectal cancer is driven by unbridled cell proliferation and an abundant extracellular matrix response with marked elevation in internal collagen levels, which are reflected on the surface and subsequently accompanied by increased amine binding sites. This indeed resulted in a 43% increase in adhesion strength in tumoral compared to healthy tissue.

The question that arises is whether there would be a similar alteration in tissue surface chemistry in a disease that originates remotely from the tissue surface, as in the case of inflammatory colitis. The inflammatory reaction of colitis is most intense at the luminal side, presenting irregular or obliterated crypts, inflammatory cell infiltrates in the lamina propria, and abscess formation at the bottom of the crypts (14). Serosal surface–interacting materials such as adhesives are thus removed from the major source of tissue alteration, yet we observed that deep tissue injury manifested as reduced amine density on the serosa compared to healthy tissue. Inflammation elicits neutrophil recruitment across the colon, starting from the mucosa and covering the serosa. As the infiltrating neutrophils release metalloproteinases, they break down collagen to allow for tissue remodeling and healing. Indeed, adhesion strength in colitic tissue with ~80% less collagen I (Fig. 2B) was 58% lower than that achieved for healthy tissue (Fig. 1D). The significant alteration of tissue surface chemistry in pathological states reiterates the importance of understanding the disease impact on the tissue microenvironment in the selection of dendrimer:dextran material formulation and also might be helpful in the design of other surface-interacting biomaterials.

Dendrimer:dextran performance was not only affected by different pathological processes, such as carcinogenesis and inflammation, but it is also affected by the state of a particular disease. For example, different severities of colitis imparted graded variation in tissue amine density and, hence, required different adhesive material formulations to achieve the desired adhesion level. We built a dataset to create a predictive model that informed on the appropriate material formulation choice given a specific colitic severity (data points plotted in Fig. 3B). The data set described adhesion strengths for three different dendrimer:dextran material formulations as a function of a range of colitis severities (measured by amine

density). A linear regression model was fit to each material formulation (Fig. 3B), and the slopes of the curves were plotted as a function of aldehyde-solid content, yielding a linear relationship (Fig. 3C). The slope of a new material formulation with a defined dextran aldehyde-solid content, 25%, was extrapolated from this fit (Fig. 3C, red triangle). The model was validated by comparing the measured adhesion strengths using a mechanical tester with the calculated ones after *ex vivo* application of the 25% solid content material formulation to tissues with three different degrees of colitis severities (Fig. 3D). As expected, there was an inverse linear correlation between disease severity and adhesion strength as a result of amine density loss (Fig. 3B). Providing more aldehyde groups to react with a tissue with low amine density can compensate for the reduction in adhesion strength resulting from collagen loss. The obtained linear relationships allowed us to construct a mathematical fit for the data, which in turn enabled us to predict the adhesion strength of a completely new dendrimer:dextran formulation when applied to either healthy, mild, or severe colitic states (Fig. 3, C and D). If this approach can be implemented in a clinical setting where a patient's colorectal biopsy can be rapidly analyzed for amine density, it would allow the surgeon to choose the optimal adhesive formulation on the basis of an individual patient's needs. This practice would help prevent material failure and improve patient outcome.

Dendrimer:dextran biocompatibility was also disease-dependent as measured by the recruitment of serosal heterophils to the interface with the adhesive material (Fig. 4, BE). Differences in disease-specific basal immunity—as evident from total inflammatory scores at tissue sites prior to injury and treatment—may explain these variable responses. Although basal immunity varies dramatically in colitic versus healthy tissue, the basal inflammatory score in the cancerous state was similar to that of a healthy state (Fig. 4, B and C). These trends correlated with the levels of heterophils recruitment upon dendrimer:dextran application compared to suture application alone (Fig. 4, C and E), being higher in colitic versus cancerous tissue. Assessing both the basal immune state as well as disease-specific immune responses was crucial to deciphering material compatibility. Healing capacity followed the same trend in both models—although our material did not affect healing in healthy tissues, application to diseased tissues improved healing capacity. This may result in part from improved mechanical stability and alleviation of local stresses imparted by the sutures when our material was applied. For both diseases, total inflammation was identical whether dendrimer:dextran was applied or not, further supporting the role of mechanical stability in the differential healing responses.

Our data reveal the profound effect of pathological states on tissue:biomaterial interactions and material performance and increase our understanding of how biological forces manifested by disease type and severity affect dendrimer:dextran adhesive performance. With a predictive model to account for those changes, we could rationally tune our material's adhesive strengths to be comparable to those of healthy tissue. Furthermore, changes in the tissue microenvironments altered dendrimer:dextran performance in our colon cancer and colitis models relative to healthy tissues, suggesting that an understanding of the diseased tissue microenvironment is key for successful translation.

An understanding of tissue:material interactions provides new vistas for materials research and characterization of therapeutic potential. Other materials and pathologies might display determinant factors that differ from those of our model adhesive hydrogel. For instance, materials that undergo oxidative degradation will degrade faster in the tumor environment as a result of an elevation in the concentration of reactive oxygen species. Similarly, natural materials that undergo enzymatic degradation will degrade differentially depending on the enzyme concentrations in an inflammatory environment relative to the basal healthy state.

Materials and Methods

Study design

The objective of this study was to investigate the effects of two pathological states [gut inflammation (colitis), in rabbits and colon neoplasia, in rats) on dendrimer:dextran adhesion (Fig. 1, C–F), biocompatibility (Fig. 4), and healing capacity (Fig. 4). With the information obtained from the adhesion studies and exploiting the tunable properties of our material, we were able to generate a data set and establish a curve fitting with the purpose of predicting material adhesion strength under a range of inflammatory states.

A linear regression model was fit to each material formulation and the slopes of the curves were plotted as a function of aldehyde solid content, yielding a linear relationship. The slope of a new material formulation with a defined dextran aldehyde solid content, 25%, was extrapolated from this fit. The model was validated by comparing the measured adhesion strengths using a mechanical tester with the calculated ones following *ex vivo* application of the 25% solid content material formulation to tissues with three different degrees of colitis severities. This model also allowed us to choose, on the basis of inflammatory disease severity, the material formulation to achieve the desired level of adhesion.

All animals (rats and rabbits) were randomly assigned to control and experimental groups, with the exception of experiments in which different strains were used as control and experimental groups (Sprague-Dawley rats as controls, which were compared with Pirc rats, an experimental model of human familial colon cancer). Sample size was determined by power analysis to achieve a minimum effect size of 0.5 with a P value of less than 0.05. Sample sizes vary between experiments and are specified in each figure caption as well as the corresponding Materials and Methods section.

Synthesis and formation of dendrimer/dextran hydrogels

Dendrimer/dextran networks were fabricated as previously described (7). Briefly, generation five polyamidoamine (PAMAM) dendrimers with 25% amine surface groups (Dendritech Inc.) were dissolved in water and mixed with a solution of oxidized dextran (50% oxidation of glucose rings, 2 aldehyde groups per oxidized glucose ring). The two homogeneous polymer solutions were loaded into a dual-chamber syringe equipped with a 8-step mixing tip. Dendrimer:dextran network formation occurred within seconds after mixing.

Fluorescent dendrimer amine

To characterize the dendrimer/dextran morphology at the tissue material interface, constituent dendrimer amine was labeled with fluorescein as previously described (7). Briefly, PAMAM dendrimer (Dendritech Inc.) was mixed with fluorescein-NHS (Life Technologies) in 50mM bicarbonate buffer for 2 hours. Then, the product was dialyzed using a 10 kDa cutoff filter and lyophilized overnight.

Colitis model in rabbits

Disease model of colitis was developed in rabbits (2.5 to 3 kg, male New Zealand White Rabbits, Charles River) by rectal instillation of 2,4-dinitrobenzenesulfonic acid (DNBS, Sigma-Aldrich). Colitis induction protocol was reviewed and approved by the Committee in Animal Care at MIT. DNBS in 25% ethanol (1 ml) was instilled through a urethral catheter introduced 15 cm into the rectum. Concentrations of DNBS were 150 and 75 mg/ml for severe and mild colitis induction, respectively. Animals were sacrificed 24 hours post-instillation and colon tissues excised.

Colon cancer model in rats

Male PIRC rats (350–400 g, retired breeder F344/NTac-Apcam1137, Taconic) were used as colorectal cancer model and male Sprague-Dawley rats (250 to 300 g, Charles River Laboratories) as control.

Tissue surface amine density

To determine the aldehyde affinity of colorectal healthy and diseased tissues, the conjugation of aldehyde-coated fluorescent microspheres (f-MS) (Molecular Probes) to tissue surfaces was quantified as previously described (7). For fluorescent microscopy purposes, tissue specimens were snap frozen overnight, cryosectioned (16-μm sections), and stained with propidium iodide (Vector Laboratories). For en face amine density quantification, sections were imaged in the Xenogen IVIS device with the appropriate filter sets (N=10 for colitis studies and N=3 for cancer studies). The fluorescence intensity was determined by calculating the efficiency overlying each construct, where the fluorescence intensity was corrected to eliminate tissue autofluorescence.

Adhesive interface morphology

To investigate the morphology of the interface between the adhesive and tissue surfaces, biopsied tissues were covered with 100 μL of fluorescently labeled dendrimer/dextran (dendrimer solution containing 0.5% tagged dendrimer) that was allowed to cure for 4 min. Tissue samples were snap frozen overnight, cryosectioned (12-μm sections), and stained with propidium iodide (Vector Laboratories). The morphology of the tissue material interface was quantified as the fluorescence intensity of fluorescein at the interface using image analysis (NIS-Elements, Nikon). The interfacial pore size and length were also measured using NIS-Elements (N=5 for each tissue type and formulation).

Adhesion mechanics

The adhesion mechanics following dendrimer/dextran application to soft tissues was measured using an Instron mechanical tester, as previously described (7). Briefly, dendrimer:dextran was applied between two uniformly sized rat colonic tissue biopsies (6 μm diameter) and allowed to polymerize for 5 min. Then, uniaxial tensile testing (Instron ElectroPuls E3000) was employed at a constant rate (0.05 mm/s) and the load response was continuously recorded to the point of macroscopic failure (*N*=5 for each tissue type and formulation).

Collagen-I immunofluorescence staining

Primary anti-collagen I antibody (Abcam) and Alexa Fluor 488 goat anti-mouse secondary antibody (Life Technologies) were used. For fluorescent microscopy purposes, tissue specimens were snap frozen overnight and cryosectioned (12-μm sections). Immunofluorescence staining against collagen I was performed using standard methods and tissues were stained with propidium iodide (Vector Laboratories). Collagen contents in the submucosa and basement membrane of the colon were quantified using image analysis (N=5 for each tissue type; NIS-Elements, Nikon). For en face collagen, tissues were processed and quantified as described for en face amine density (N=10 for colitis studies and N=3 for cancer studies).

TNF-α immunofluorescence staining

Primary anti-TNF-α antibody (Santa Cruz Biotechnology) and goat anti-rabbit IgG fluorescein conjugate secondary antibody (EMD Millipore) were used. Tissue specimens processed as described for collagen immunofluorescence staining. TNF-α content in the colonic mucosa was quantified using image analysis (*N*=5 for each tissue type; NIS-Elements, Nikon).

Neutrophil immunofluorescence staining

Primary anti-MAC-387 (FITC) antibody (Abcam) was used, which recognizes the Calprotectin molecule, an intra-cytoplasmic antigen expressed by granulocytes, monocytes and tissue macrophages. Tissue specimens were processed as described for collagen immunofluorescence staining. Neutrophil recruitment to the submucosa and basement membrane of the colon was quantified using image analysis (*N*=5 for each tissue type; NIS-Elements, Nikon).

Enterotomy procedure

Enterotomy procedures were performed in both models of colitis and colon cancer, as well as in healthy controls, by creating an incision in the colon and applying sutures to the anastomoses site with or without the application of dendrimer:dextran adhesive material. Enterotomy studies were reviewed and approved by the Committee in Animal Care at MIT. Harvested tissue was excised a week post-surgery and cryosectioned to create 10-μm-thick sections. Hematoxylin and eosin staining was performed using standard methods. Histological slides were evaluated for their extent of inflammation, serosal heterophils and serosal fibrosis using the following scores: 0, no observable change compared to the control;

1, a nearly imperceptible feature (minimal); 2, an easily identifiable or notable (mild/moderate) feature; 3, a prominent to overwhelming (marked/severe) feature (N=5 for each experimental group).

Statistical analyses

Data are presented as mean ± standard deviation. Graphs were created using GraphPad Prism software. All statistical comparisons were performed with a two-tailed t-test for independent samples using VassarStats software (Vassar College, Poughkeepsie, NY, USA). A P value of <0.05 was considered to denote statistical significance. Data marked with the same symbol (for example, single asterisk or double asterisk) represent values with statistical significance between them.

Supplementary Material

Refer to Web version on PubMed Central for supplementary material.

Acknowledgments

We thank the histology core facility at the MIT Division of Comparative Medicine and the imaging core facility at the MIT Koch Institute for Integrative Cancer Research.

Funding: Supported by RO1 grant (GM49039) and MIT Deshpande Center for Technological Innovation.

References

1. Cam C, Segura T. Matrix-based gene delivery for tissue repair. Current Opin in Biotechnol. 2013; 24:855–863.
2. Orive G, Santos E, Pedraz JL, Hernandez RM. Application of cell encapsulation for controlled delivery of biological therapeutics. Advanced Drug Delivery Rev. Jul 23.2013 10.1016/j.addr.2013.07.009
3. Armentano I, Fortunati E, Mattioli S, Rescignano N, Kenny JM. Biodegradable composite scaffolds: A strategy to modulate stem cell behaviour. Recent Pat Drug Deliv Formul. 2013; 7:9–17. [PubMed: 23017149]
4. Saiz E, Zimmermann EA, Lee JS, Wegst UG, Tomsia AP. Perspectives on the role of nanotechnology in bone tissue engineering. Dental Mater. 2013; 29:103–115.
5. Orlando G, Bendala JD, Shupe T, Bergman C, Bitar KN, Booth C, Carbone M, Koch KL, Lerut JP, Neuberger JM, Petersen B, Ricordi C, Atala A, Stratta RJ, Soker S. Cell and organ bioengineering technology as applied to gastrointestinal diseases. Gut. 2013; 62:774–786. [PubMed: 22267591]
6. Brown BN, Badylak SF. Expanded applications, shifting paradigms and an improved understanding of host-biomaterial interactions. Acta Biomaterialia. 2013; 9:4948–4955. [PubMed: 23099303]
7. Oliva N, Shitreet S, Abraham E, Stanley B, Edelman ER, Artzi N. Natural tissue microenvironmental conditions modulate adhesive material performance. Langmuir. 2012; 28:15402–15409. [PubMed: 23046479]
8. Artzi N, Shazly T, Baker AB, Bon A, Edelman ER. Aldehyde-amine chemistry enables modulated biosealants with tissue-specific adhesion. Adv Mater. 2009; 21:3399–3403. [PubMed: 20882504]
9. Artzi N, Shazly T, Crespo C, Ramos AB, Chenault HK, Edelman ER. Characterization of star adhesive sealants based on PEG/dextran hydrogels. Macromolecular Biosci. 2009; 9:754–765.
10. Graham MF, Diegelmann RF, Elson CO, Lindblad WJ, Gotschalk N, Gay S, Gay R. Collagen content and types in the intestinal strictures of Crohn's disease. Gastroenterology. 1988; 94:257–265. [PubMed: 3335305]

11. Cury DB, Mizsputen SJ, Versolato C, Miiji LO, Pereira E, Delboni MA, Schor N, Moss AC. Serum calprotectin levels correlate with biochemical and histological markers of disease activity in TNBS colitis. Cellular Immunol. 2013; 282:66–70. [PubMed: 23685388]

12. Mowat AM, Bain CC. Mucosal macrophages in intestinal homeostasis and inflammation. J Innate Immunity. 2011; 3:550–564. [PubMed: 22025201]

13. Lenglet S, Mach F. Montecucco, Role of matrix metalloproteinase-8 in atherosclerosis. Mediators Inflamm. Jan 9.2013 10.1155/2013/659282

14. Morimoto Y, Tanaka K, Toiyama Y, Inoue Y, Araki T, Uchida K, Kimura K, Mizoguchi A, Kusunoki M. Intravital three-dimensional dynamic pathology of experimental colitis in living mice using two-photon laser scanning microscopy. J Gastrointestinal Surg. 2011; 15:1842–1850.

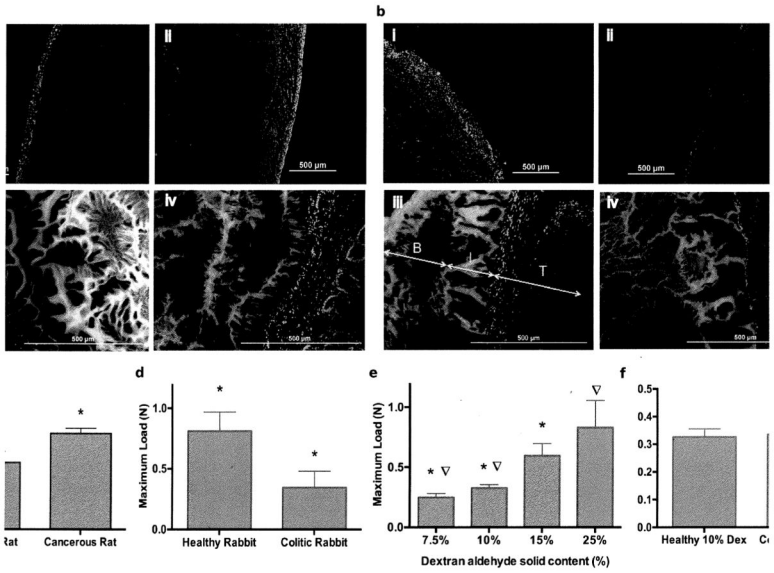

Fig. 1. Assessment of tissue:material interactions and mechanical properties as a function of disease type

(A) Amine density on colon serosal layer was assessed by aldehyde-coated fluorescent microspheres (green) in rat healthy (i) and cancerous (ii) tissues (red, stained with propidium iodide); and dendrimer:dextran adhesive (green, tagged with fluorescein) morphology when applied to rat healthy (iii) and neoplastic (iv) tissues (red, stained with propidium iodide). (B) Aldehyde-coated fluorescent microspheres (green) and dendrimer:dextran morphology (green, tagged with fluorescein) applied to rabbit healthy (I and iii) and inflamed (ii and iv) tissues (red, stained with propidium iodide). Maximum load at failure measured for (C) healthy and cancerous tissues and (D) healthy and inflamed tissues. (E) Maximum load at failure measured for different material formulations (dextran aldehyde solid contents from 7.5 to 25% with fixed dendrimer amine solid content of 20%) on healthy rabbit colon ($P<0.05$). Dextran aldehyde solid content can be tuned to match the surface amine density of the target tissue. (D) By increasing dextran aldehyde solid content from 10% to 25%, statistically equal levels of adhesion can be achieved in healthy and inflamed tissues, respectively. For all mechanical testing data, $N=5$ for each experimental group. In each graph, data marked with the same symbol represents statistical significance with $P<0.05$.

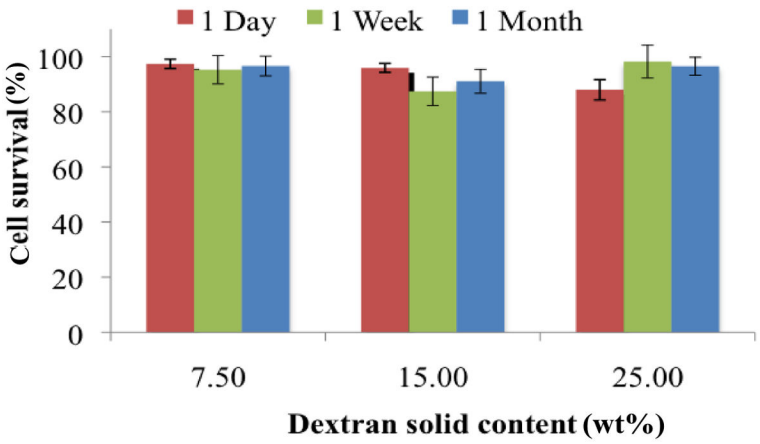

Fig. 2. Affect of colitis on collagen I content transluminally

Amine density and surface collagen content were quantified en face using aldehyde coated fluorescent microspheres and anti-collagen I antibody, respectively, in (A) healthy and cancerous rat tissues (N =3 for each experimental group) and (B) healthy and colitic rabbit tissues (N=10 for each experimental group). (C) High correlation is achieved between collagen and amine density en face (R^2=0.99, P< 0.05). In each graph, data marked with the same symbol represents statistical significance with P<0.05.

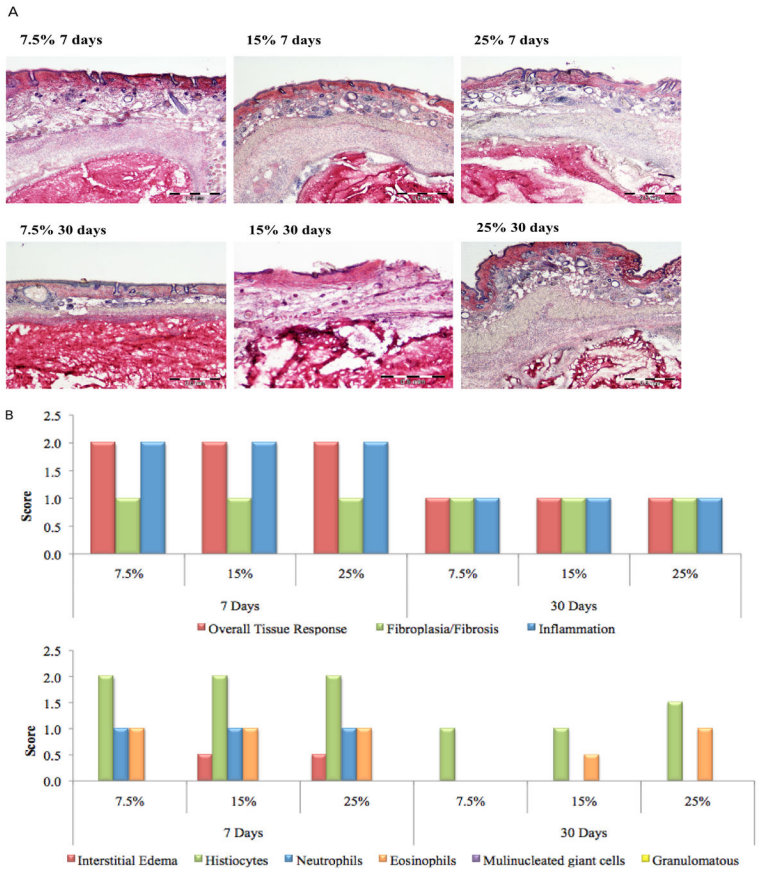

Fig. 3. Effect of disease severity on material performance

(A) Immunofluorescence staining against collagen, both for basement membrane collagen (cryosection staining, i to iii) and serosal collagen (en face staining, iv–vi), was performed in rabbits using healthy, mild and severe colitic tissues. (B) Maximum load at failure as a function of amine density and hence, inflammation severity, for a range of material formulations (D10, 15, 20 represent dextran aldehyde with 10, 15, or 20% solid content, and G20 is PAMAM dendrimer 20% solid content; *N*=20 of varying degrees of inflammation for each adhesive formulation). (C) The slopes of the curve fits for maximum load at failure as a function of inflammation severity linearly correlate with dextran aldehyde solid content (10, 15, and 20%). This correlation was used to predict the slope for a new dextran solid content of 25% (D25, red triangle in the graph). (D) Experimental (measured) and predicted (calculated using model) adhesion strengths of a new formulation (D25 and G20) applied to three tissue samples spanning a range of inflammatory severities (*N*=1 for each inflammation severity).

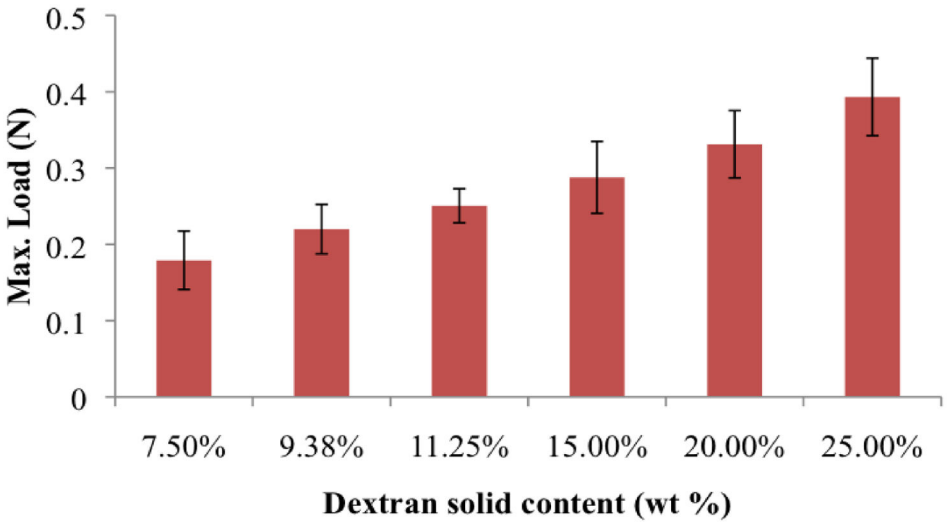

Fig. 4. Adhesive-mediated healing capacity

(A) Hematoxylin and eosin (H&E) staining of (i) healthy and (ii) cancerous rat tissues and (iii) healthy and (iv) inflammed rabbit tissues following incision, suturing and adhesive application. Histological scoring of inflammation, serosal heterophils, and serosal fibrosis in the case of (B) healthy and (C) cancerous rat tissues and (D) healthy and (E) colitic rabbit tissues (N=5 for each experimental group). In each graph, data marked with the same symbol represents statistical significance, with P<0.05.